oe4625 Dredge Pumps and Slurry Transport

Vaclav Matousek
October 13, 2004

TU Delft
Delft University of Technology

1. BASIC PRINCIPLES OF FLOW IN PIPE

SOLID PARTICLES IN QUIESCENT LIQUID

SOLID PARTICLES IN FLOWING LIQUID

PARTICLES IN LIQUID

BUOYANCY

DRAG

LIFT

TURBULENT DISPERSION

INTERPARTICLE CONTACTS

SOLID PARTICLE IN QUIESCENT LIQUID

Terminal settling velocity of sphere

Terminal settling velocity of non-spherical particle
(*particle shape effect***)**

Hindered settling velocity of particle in cloud
(*solids concentration effect***)**

Terminal Settling Velocity of Sphere

Forces acting on a solid spherical particle submerged in a quiescent water column:

Gravitational force: $F_g = \dfrac{\pi d^3}{6} \rho_s g$ [N]

Buoyancy force: $F_b = \dfrac{\pi d^3}{6} \rho_f g$ [N]

Drag force: $F_D = fn(\rho_f, \mu_f, d, v_{ts})$ [N]

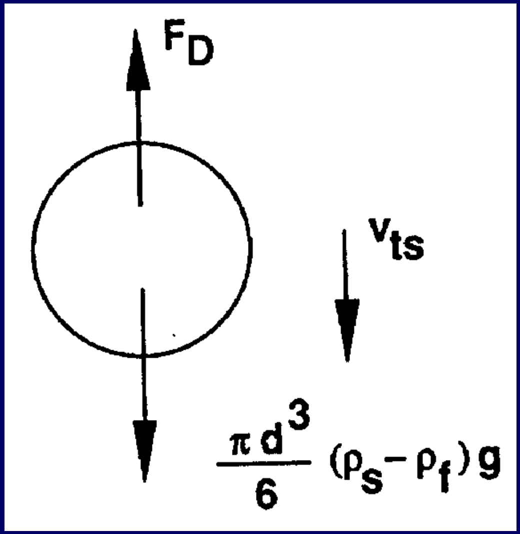

The balance of the three forces acting on the submerged solid body determines the settling velocity, v_{ts}, of the body.

Terminal Settling Velocity: Buoyancy Force

Example: The hydrostatic force acts on the top and the bottom of a solid cylinder submerged in the liquid.

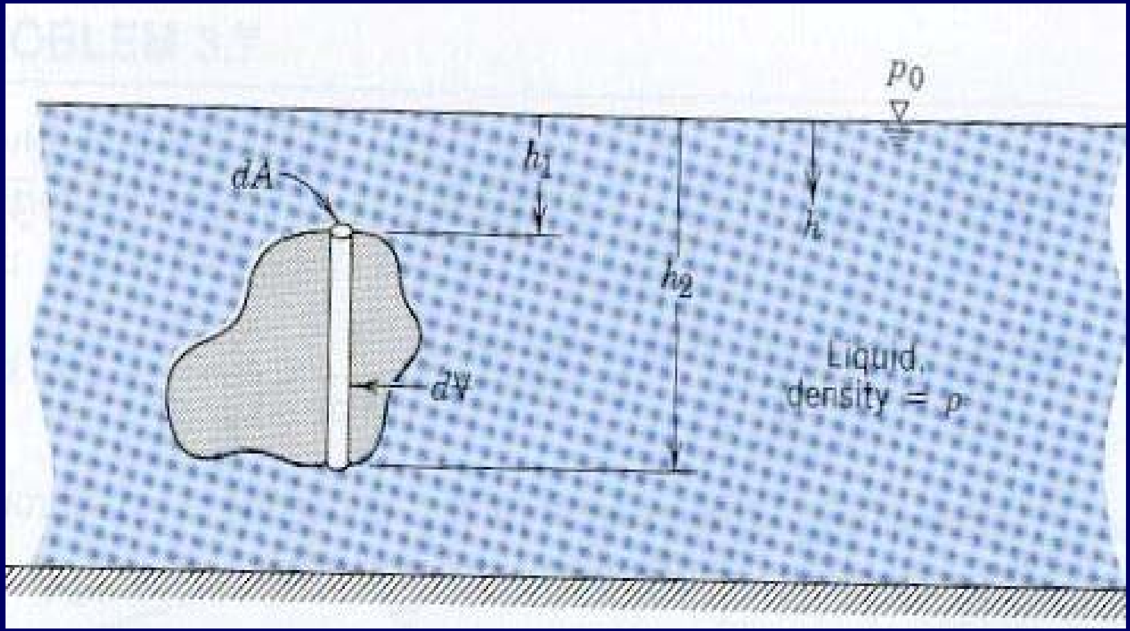

Top of cylinder:

Force downwards

$F_{top}=(p_0+h_1\rho_f g)dA$

Bottom of cylinder:

Force upwards

$F_{bot}=-(p_0+h_2\rho_f g)dA$

Buoyancy force: $F_{top}+F_{bot}=\rho_f g\ (h_1-h_2)dA=-\rho_f g Volume_{cylind}$

Drag Force

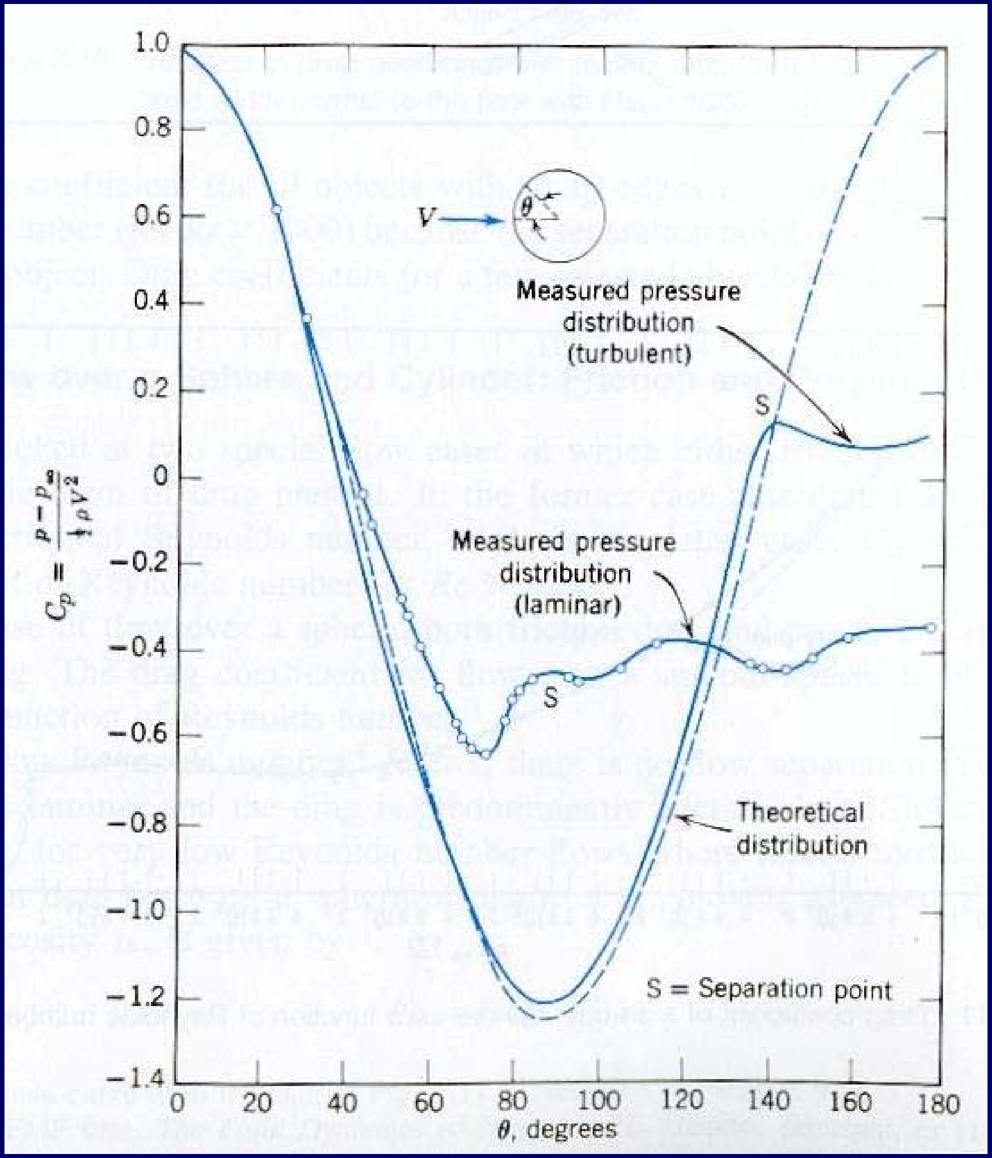

- The drag force is a product of the pressure differential developed over a sphere due to the flow round the sphere.
- Total drag is composed of skin-friction drag and pressure drag.

Figure: Pressure distribution around a smooth sphere for laminar and turbulent-layer flow, compared with theoretical inviscid flow.

TU Delft

Terminal Settling Velocity: Drag Force

The pattern of the flow round a particle (sphere) is characterized by developments in the **boundary layer** (BL) at the particle surface. The BL can be laminar or turbulent.

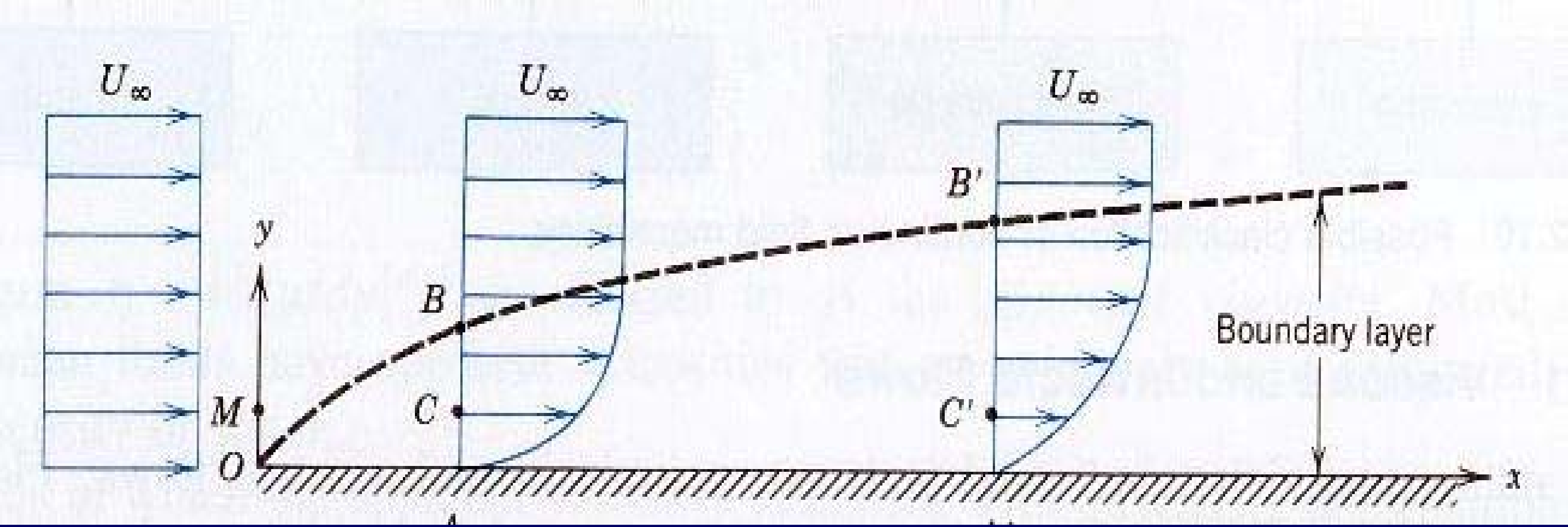

Terminal Settling Velocity: Drag Force

Drag acting on a solid particle (sphere) depends on a development of flow in the boundary layer. Flow separation and with the separation associated development of a turbulent wake affect the drag force.

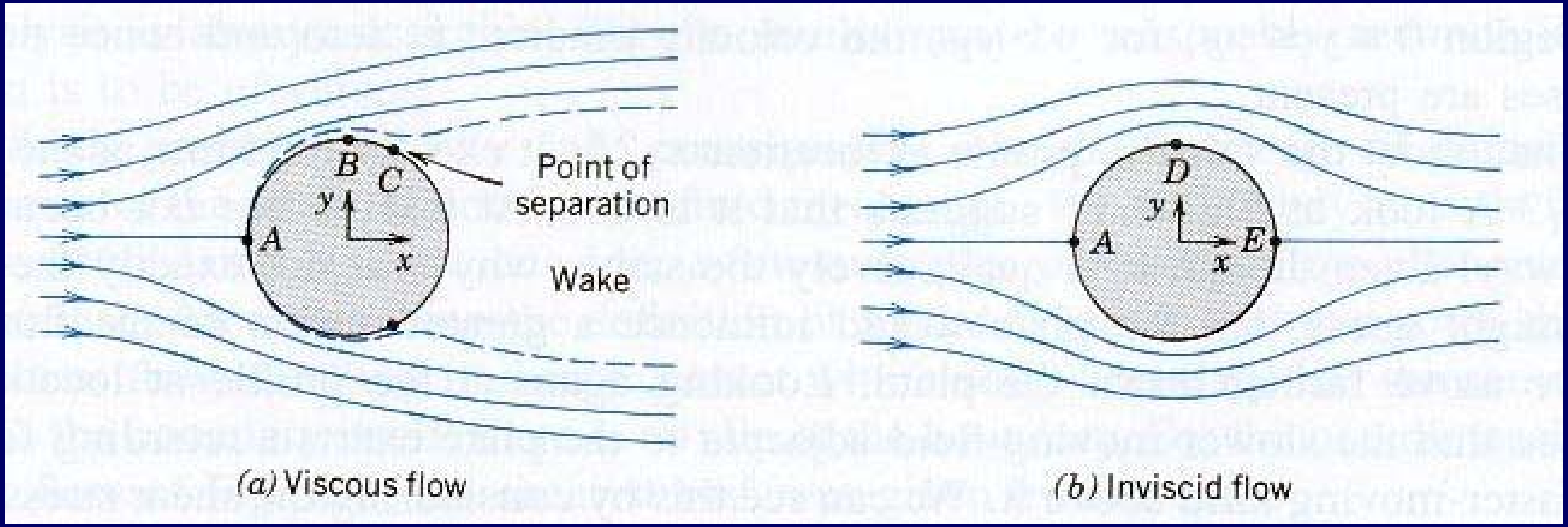

TUDelft

Terminal Settling Velocity: Drag Force

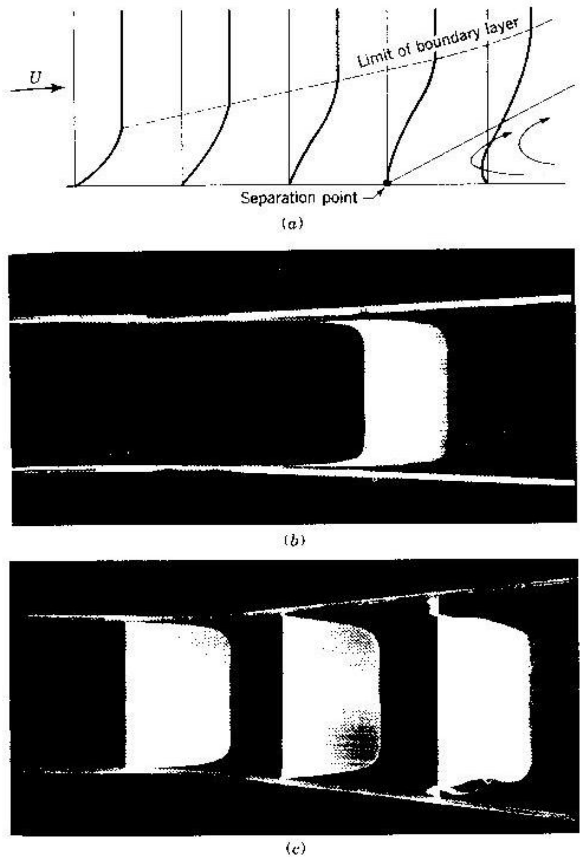

Figure 5.18 (*a*) Effect of adverse pressure gradient on boundary layer. Separation. (*b*) Boundary-layer growth in a small-angle diffuser. (*c*) Boundary-layer separation in a large-angle diffuser. [*Parts (b) and (c) from the film "Fundamentals of Boundary Layers," by the National Committee for Fluid Mechanics Films and the Education Development Center.*]

- **Separation** of flow from the sphere surface can occur as a result of the adverse pressure gradient (dp/dx > 0). The separation increases pressure drag on sphere.
- The effect of separation is to decrease the net amount of flow work that can be done by a fluid element on the surrounding fluid at the expense of its kinetic energy, with the net result that pressure recovery is incomplete and flow losses (drag) increase.

TU Delft

Terminal Settling Velocity: Drag Force

The dimensional analysis of **$F_D = fn(\rho_f, v_{ts}, \mu_f, d)$** provides two dimensionless groups:

$$C_D = \frac{8F_D}{\pi d^2 v_{ts}^2 \rho_f} = \frac{drag.force}{hydrodynamic.force}$$

$$\mathrm{Re}_p = \frac{v_{ts} d \rho_f}{\mu_f} = \frac{inertia.force}{viscous.force}$$

The relationship **$C_D = fn(\mathrm{Re}_p)$** is determined experimentally.

Terminal Settling Velocity: Drag Force

The relationship $C_D = fn(Re_p)$ is determined experimentally: v_{ts} for a spherical particle is measured.

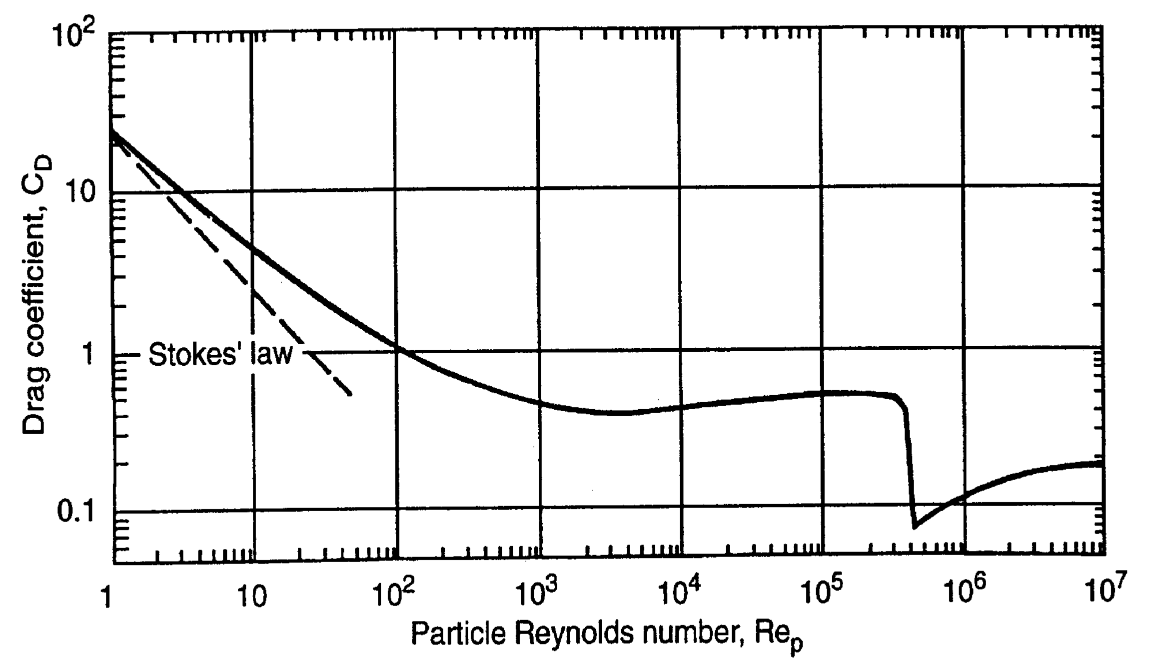

Regimes

Laminar: $Re_p < 1$

$C_D = 24/Re_p$

Transitional:

$C_D = fn(Re_p)$

Turbulent:

$3 \times 10^5 > Re_p > 500$

$C_D = 0.445$.

Terminal Settling Velocity: Drag Force

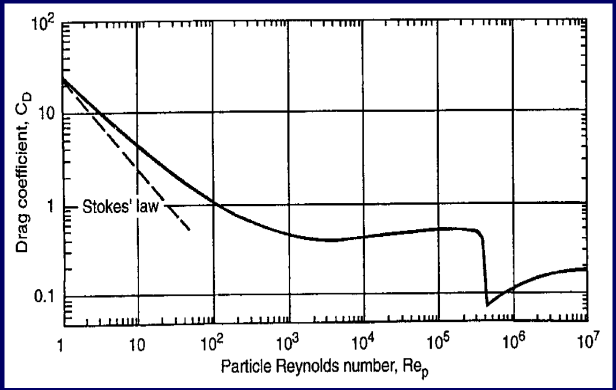

Laminar regime: Re_p<1 (Stokes flow):

- laminar flow round a sphere, no flow separation from a sphere; wake is laminar
- drag is predominantly due to friction
- pressure differential due to viscosity between the forward (A) and rearward (E) stagnation points: p(A) > p(E)

Terminal Settling Velocity: Drag Force

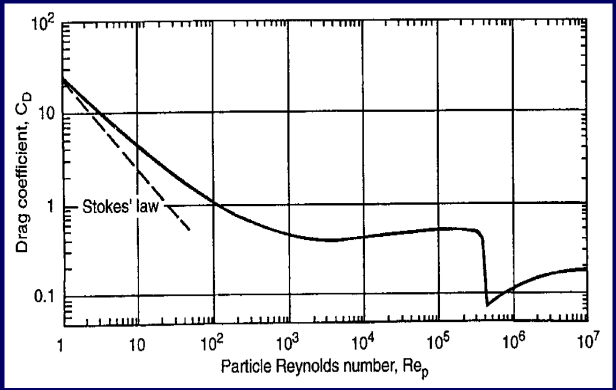

Transitional regime: $1000 > Re_p > 1$:

- the flow separates and forms vortices behind the sphere;
- drag is a combination of friction and pressure drag

Terminal Settling Velocity: Drag Force

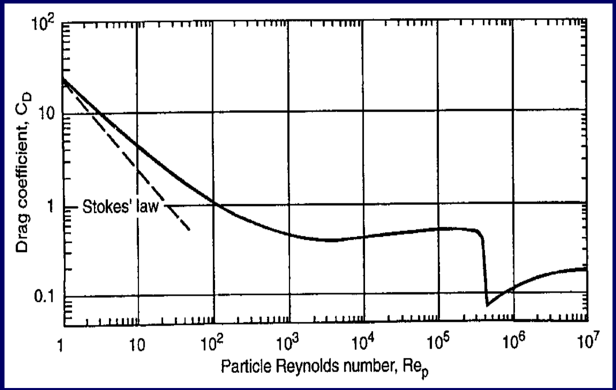

Inertial regime: $3x10^5 > Re_p > 10^3$:

- the boundary layer on the forward portion of the sphere is laminar; separation occurs just upstream of the sphere midsection; wide turbulent wake downstream
- the pressure p(E) in the separated region is almost constant and lower than p(A) over the forward portion of the sphere
- drag is primarily due to this pressure differential, no viscous effect

Terminal Settling Velocity: Drag Force

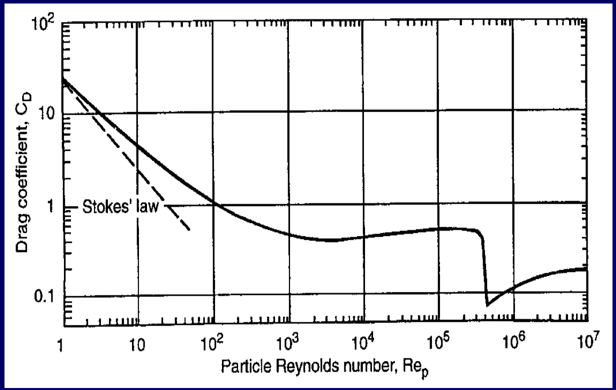

Critical $Re_p \sim 3 \times 10^5$:

- the boundary layer becomes turbulent and the separation point moves downstream, wake size is decreased
- the pressure differential is reduced and C_D decreases abruptly;
- rough particles – turbulence occurs at lower Re_p, thus $Re_{p,cr}$ is reduced.

Turbulent boundary layer has more momentum than laminar BL and can better resist an adverse pressure gradient. It delays separation and thus reduces the pressure drag.

Terminal Settling Velocity: Drag Force

Streamlined bodies are so designed that the separation point occurs as far down-stream as possible. If separation can be avoided the only drag is skin friction.

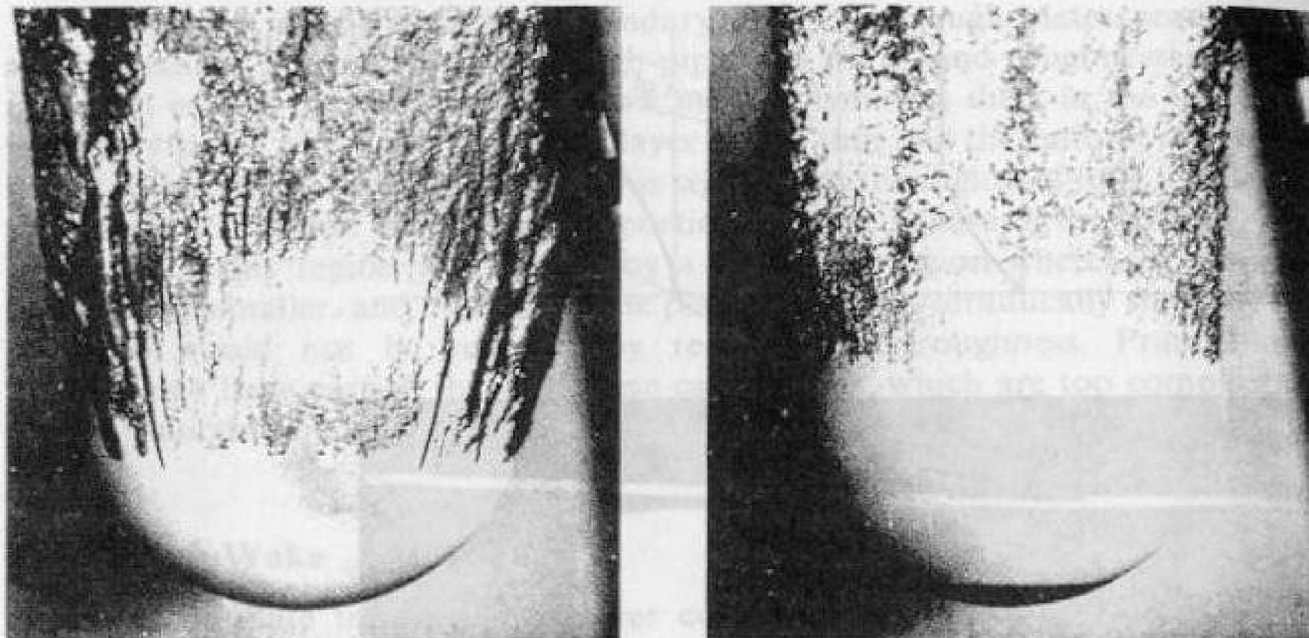

(*a*) (*b*)

Figure 5.20 Shift in separation point due to induced turbulence: (*a*) 216 mm bowling ball, smooth surface, 7.62 m/s entry velocity into water; (*b*) same except for 100 mm diameter patch of sand on nose. (*Official U.S. Navy photograph made at Navy Ordnance Test Station, Pasadena Annex.*)

Drag coefficient, C_D

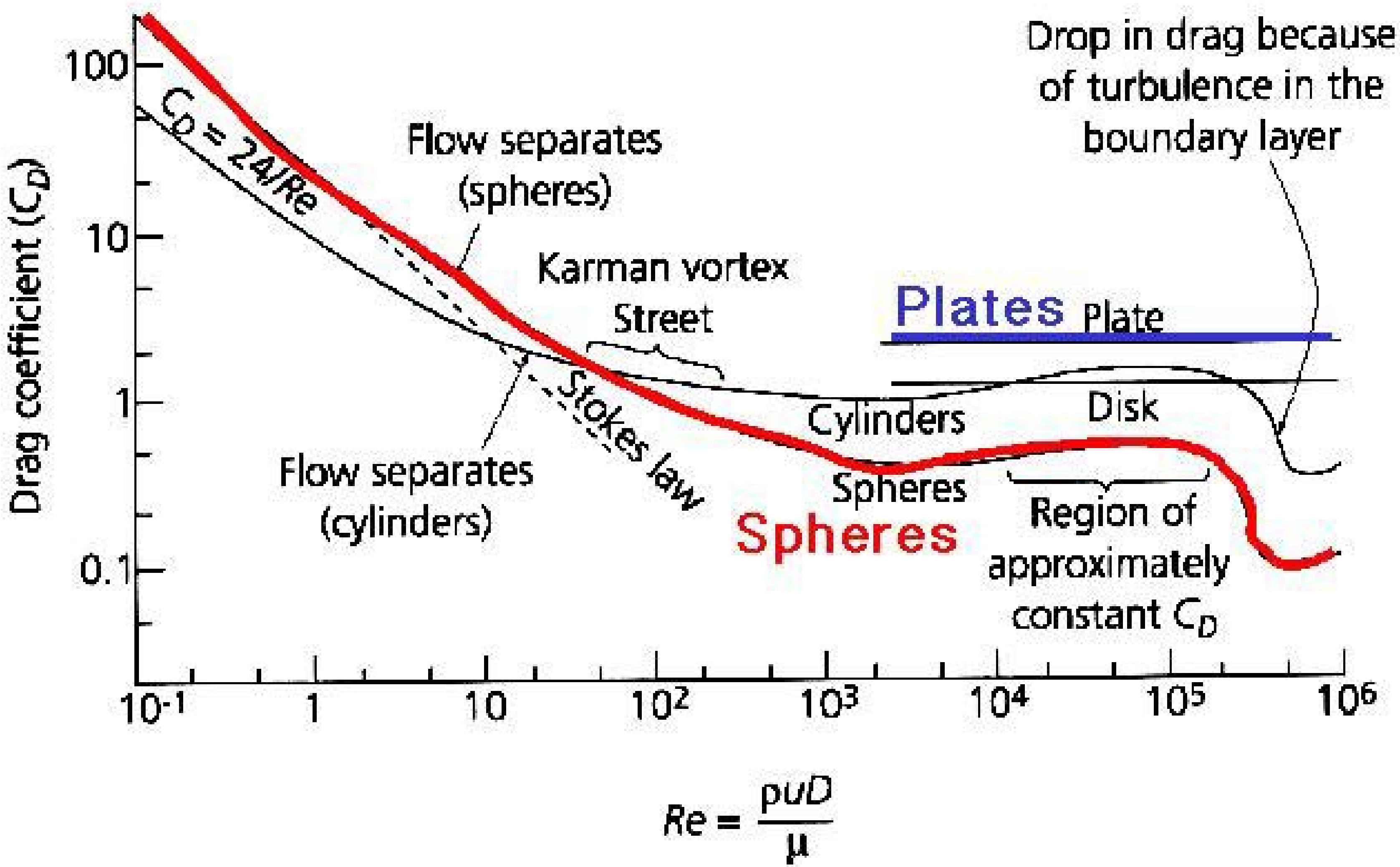

Terminal Settling Velocity of Sphere

The balance of the gravitational, buyoancy and drag forces

$$\frac{\pi d^3}{6}\left(\rho_s - \rho_f\right) g = \frac{C_D}{8} \pi d^2 v_{ts}^2 \rho_f \qquad [N]$$

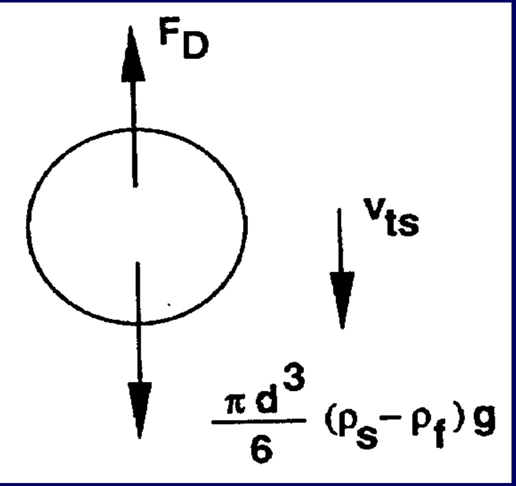

produces an eq. for the terminal settling velocity of a spherical particle, v_{ts}

$$v_{ts} = \sqrt{\frac{4}{3}\frac{\left(\rho_s - \rho_f\right)}{\rho_f}\frac{gd}{C_D}} \qquad [m/s].$$

The v_{ts} formula is an implicit equation and must be solved iteratively for settling in the transitional regime.

TU Delft

Terminal Settling Velocity of Sphere

In the ***laminar regime*** (obeying the Stokes' law, Rep < 0.1, i.e. sand-density particles of d < 0.05 mm approximately)

$C_D = 24/Re_p$, so that

$$v_{ts} = \frac{\left(\rho_s - \rho_f\right)}{18} \frac{gd^2}{\mu_f}$$

In the ***turbulent regime*** (obeying the Newton's law, Rep >500, i.e. sand-density particles of d > 2 mm approximately) $C_D = 0.445$, and

$$v_{ts} = 1.73\sqrt{\frac{\left(\rho_s - \rho_f\right)}{\rho_f} gd}$$

Terminal Settling Velocity of Sphere

The two regimes are connected via the ***transition regime***, <u>$C_D = fn(Re_p)$</u>.
The determination of v_{ts} requires an iteration.

Grace (1986) proposed a method for a determination of v_{ts} *without necessity to iterate*. The <u>Grace method</u> uses two dimensionless parameters

$$d^* = d.\sqrt[3]{\frac{\rho_f\left(\rho_s-\rho_f\right)g}{\mu_f^2}}$$

$$v_{ts}^* = v_{ts}\sqrt[3]{\frac{\rho_f^2}{\mu_f\left(\rho_s-\rho_f\right)g}}$$

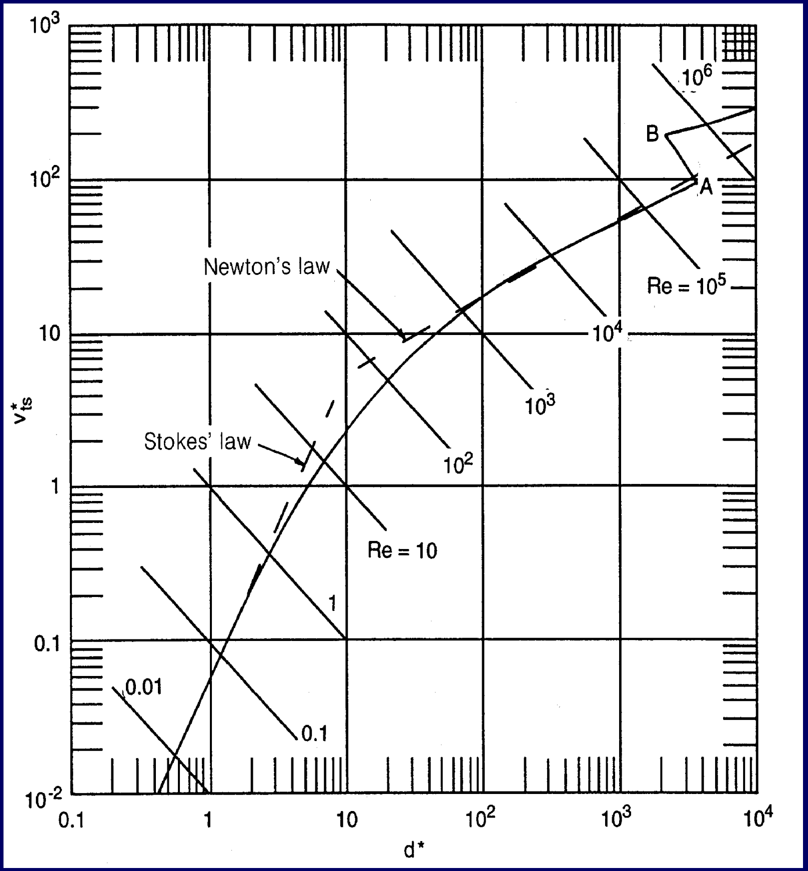

Terminal Settling Velocity of non-S Particle

The **non-spherical shape of a particle** reduces its settling velocity. This can be quantified by the velocity ratio called the shape factor.

$$\xi = \frac{v_t}{v_{ts}}$$

The shape factor is a function of :

- the volumetric form factor k (k=0.26 for sand, gravel)
- the dimensionless particle diameter, d*

$$d^* = d \cdot \sqrt[3]{\frac{\rho_f \left(\rho_s - \rho_f\right) g}{\mu_f^2}}$$

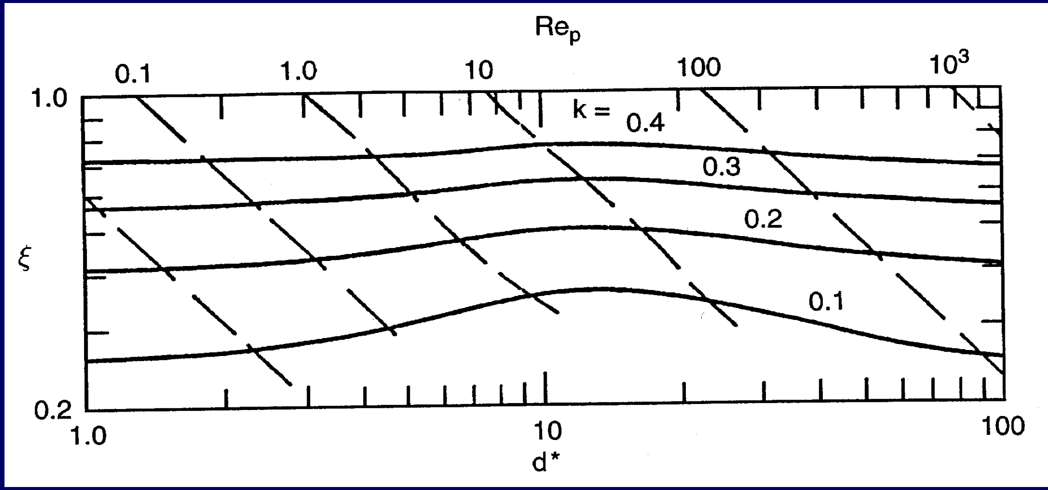

The terminal velocity for sand particles is typically 50-60 % of the value for the sphere of the equivalent diameter.

Terminal Settling Velocity of Sand Particle

In the ***laminar regime*** (sand particles smaller than 0.1 mm) the Stokes equation :

$$v_t = 424 \frac{\left(S_s - S_f\right)}{S_f} d^2$$

In the ***transition regime*** (0.1 mm<d< 1 mm) the Budryck equation :

$$v_t = \frac{8.925}{d} \sqrt{1 + 95 \frac{\left(S_s - S_f\right)}{S_f} d^3 - 1}$$

In the ***turbulent regime*** (sand particles larger than 1 mm) the Rittinger equation :

$$v_t = 87 \sqrt{\frac{\left(S_s - S_f\right)}{S_f} d}$$

Remark: input d in [mm], output v_t in [mm/s].

Terminal Settling Velocity of Sand Particle

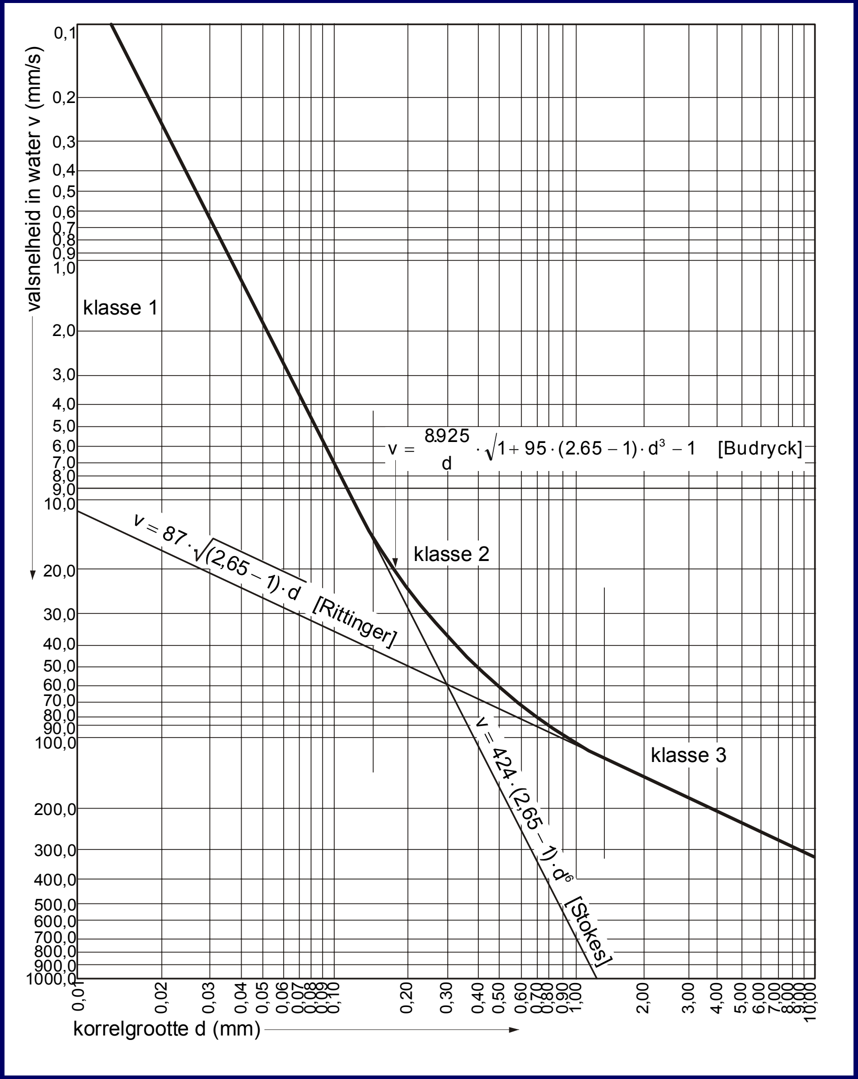

Terminal settling velocity of sand & gravel particles using Stokes, Budryck and Rittinger equations.

Hindered Settling Velocity of Particle

When a cloud of solid particles settles in a quiescent liquid additional hindering effects influence the **settling velocity, v_{th}**, of particles in the cloud:

•the increased buoyancy due to the presence of other particles at the same vertical level

•the upflow of liquid as it is displaced by the descending particles, and

•the increased drag caused by the proximity of particles within the cloud.

The hindering effects are strongly dependent on the volumetric concentration of particles in the cloud, Cv, and described by

the Richardson & Zaki equation for which the Wallis eq. determines the index m

$$v_{th} = v_t \left(1 - C_v\right)^m$$

$$m = \frac{4.7\left(1 + 0.15\,\mathrm{Re}_p^{0.687}\right)}{1 + 0.253\,\mathrm{Re}_p^{0.687}}$$

SOLID PARTICLE IN FLOWING LIQUID

Particle – liquid interaction:

Hydrodynamic lift

Turbulent dispersion

Particle – particle interaction:

Permanent contact

Sporadic contact

Particle-Liquid Interaction: Lift

The lift force, F_L, on a solid particle is a product of simultaneous ***slip*** (given by relative velocity $v_r = v_f - v_s$) and ***particle rotation***. The velocity differential between liquid velocities above and below the particle produces a pressure differential in the vertical direction over the particle and thus the **vertical force**.

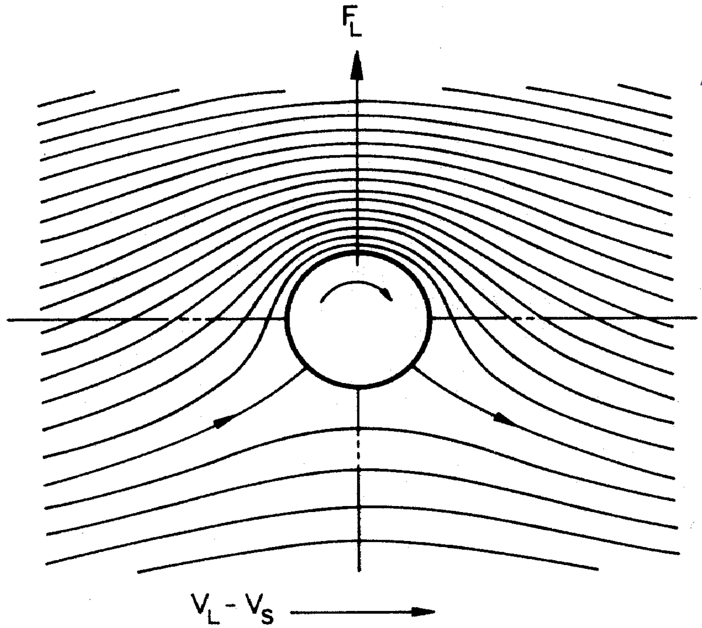

A. Magnus lift due to external rotation

B. B. Saffman lift due to velocity gradient

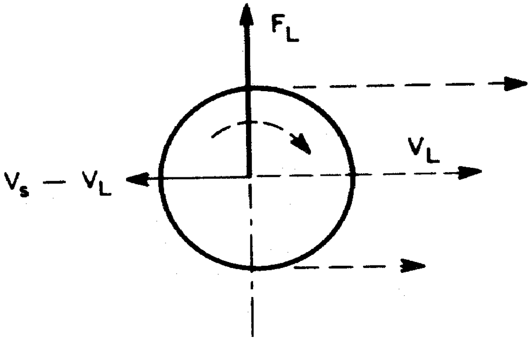

Particle-Liquid Interaction: Lift

The Saffman lift force: $F_{Saff} = 1{,}61 \cdot \mu_f \cdot D \cdot \left|u_r\right| \cdot \sqrt{Re_G}$

with the shear Reynolds number: $Re_G = \frac{\rho_f D^2}{\mu_f} \cdot \frac{du}{dy}$

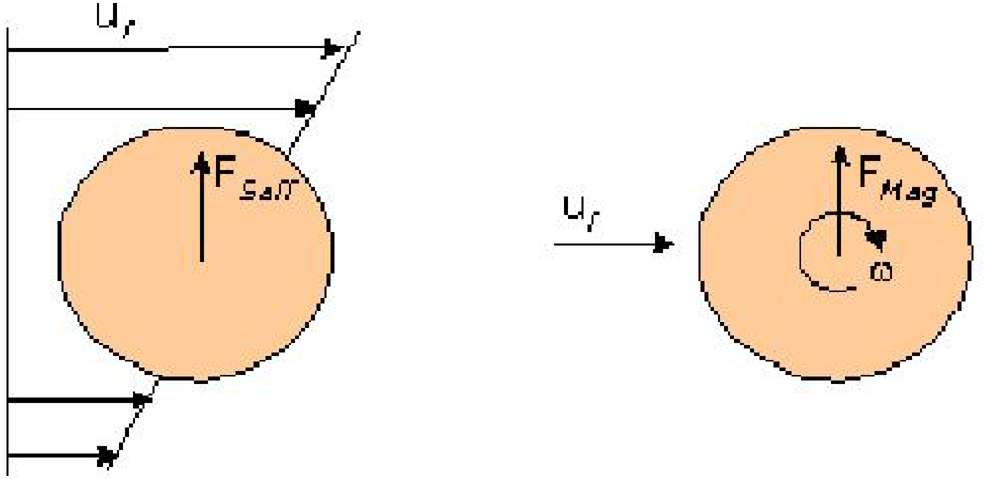

Saffman lift

Magnus lift

The Magnus lift force:

$$F_{Mag} = \frac{1}{2} \cdot \rho_f \cdot \left|u_r\right| \cdot C_{LR} \cdot A \cdot \left(\frac{u_r \times \omega_r}{\omega_p - \frac{1}{2} \nabla \times u_f} \right)$$

with the lift coefficient:

$$C_{LR} = \frac{D \cdot \left|\omega_p\right|}{\left|u_r\right|}$$

Lift Application: Initiation of Sediment Motion

Driving forces:

- Drag
- Buoyancy
- Lift
- Downslope weight

Resisting forces:

- Particle weight (gravity)
- Grain packing

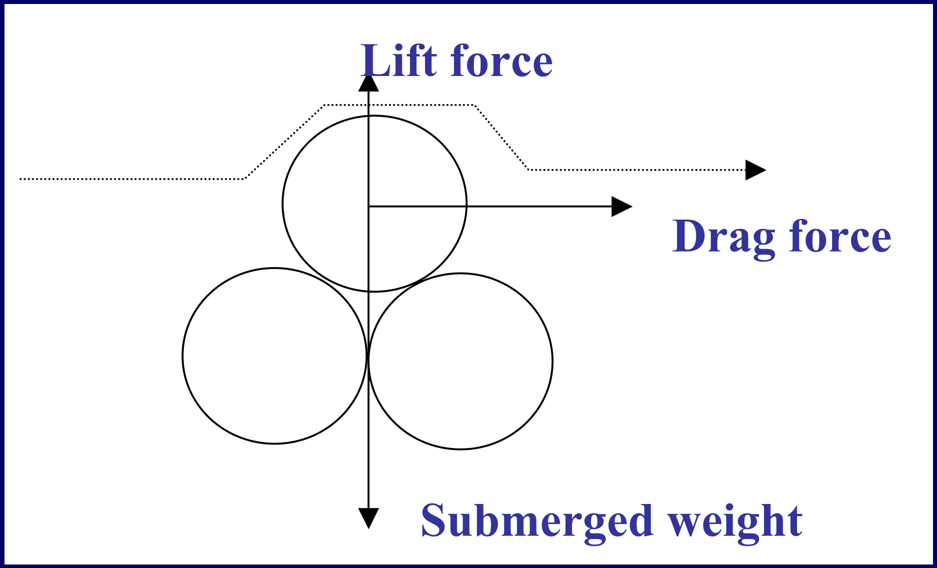

Particle-Liquid Interaction: Turb Dispersion

An intensive exchange of momentum and random velocity fluctuations in all directions are characteristic of the turbulent flow of the carrying liquid in a pipeline.

A turbulent eddy is responsible for the transfer of momentum and mass in a liquid flow. The length of the turbulent eddy is called the mixing length.

The turbulent fluctuating component v' of the liquid velocity v is associated with a turbulent eddy.

Turbulent eddies are responsible for solid particle suspension. The ability of a carrying liquid to suspend the particles is determined by

- the intensity of liquid turbulence (depends on liquid velocity)
- the size of the turbulent eddy (depends on pipe diameter)
- the size of the solid particle.

Particle-Liquid Interaction: Turb Dispersion

Turbulent diffusion model of Schmidt and Rouse

The model is a balance of upwards and downwards solids fluxes composed of the volumetric settling rates and the diffusion fluxes:

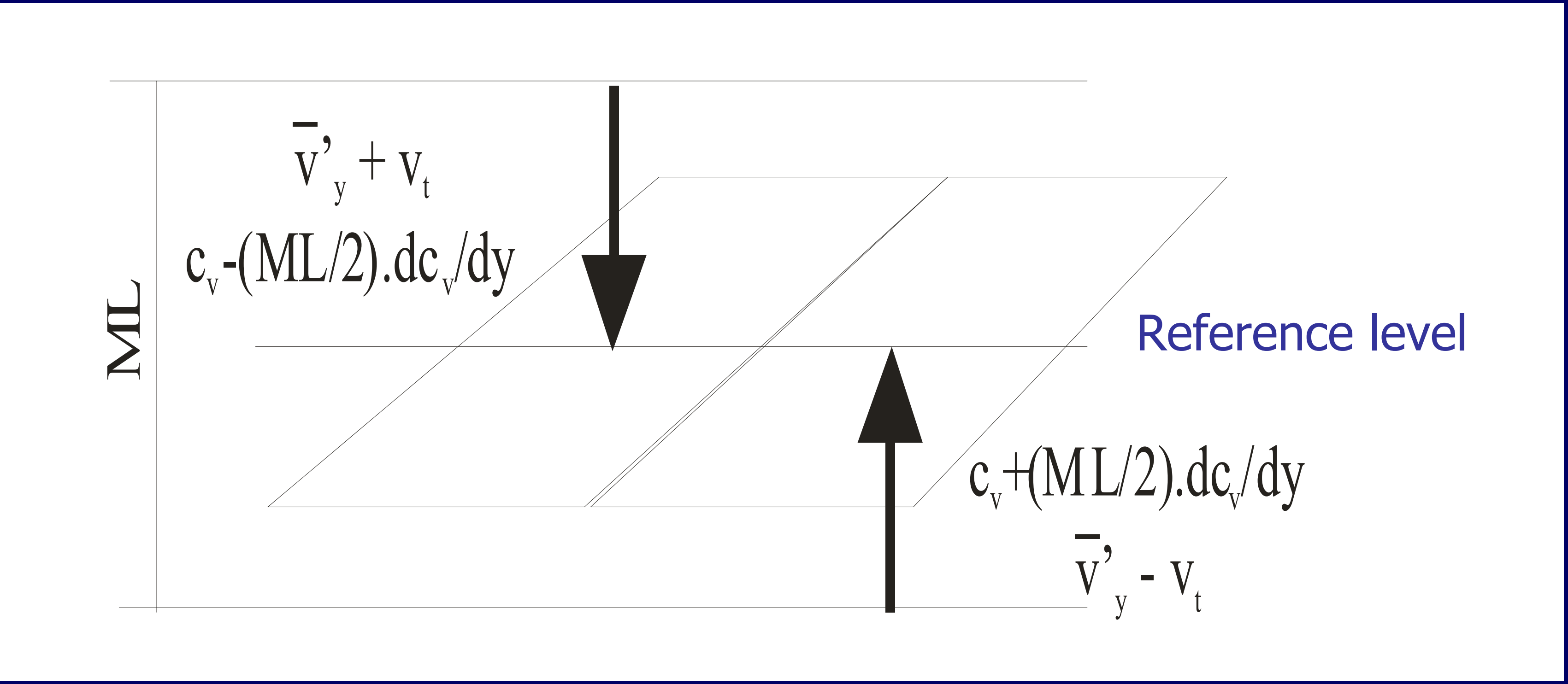

Particle-Liquid Interaction: Turb Dispersion

Turbulent diffusion model of Schmidt and Rouse

The model is a balance of upwards and downwards solids fluxes composed of the volumetric settling rates and the diffusion fluxes:

The upwards flux per unit area = The downwards flux per unit area

$$\frac{1}{2}\left[c_v+\left(\frac{ML}{2}\right)\frac{dc_v}{dy}\right]\left(\tilde{v}'_y-v_t\right) = \frac{1}{2}\left[c_v-\left(\frac{ML}{2}\right)\frac{dc_v}{dy}\right]\left(\tilde{v}'_y+v_t\right)$$

gives $$-\varepsilon_s\frac{dc_v}{dy}=v_t.c_v$$ where $$\varepsilon_s=\frac{ML}{2}\tilde{v}'_y$$

and the integration provides

$$c_v(y)=C_{vb}.\exp\left[-\frac{v_t}{\varepsilon_s}\left(y-y_b\right)\right]$$

Real Turbulent-Suspension Profiles

Medium sand in a 150-mm pipe (horizontal):

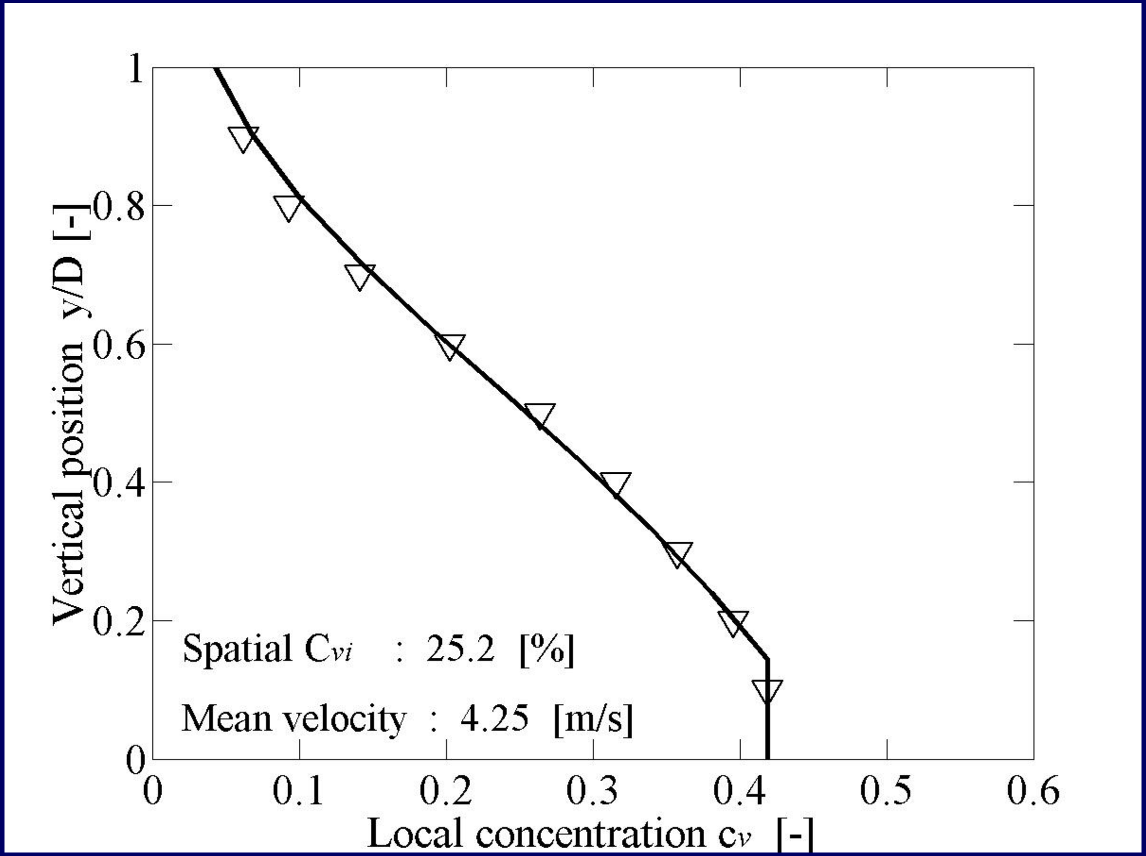

Real Turbulent-Suspension Profiles

Medium sand in a 150-mm pipe (horizontal):

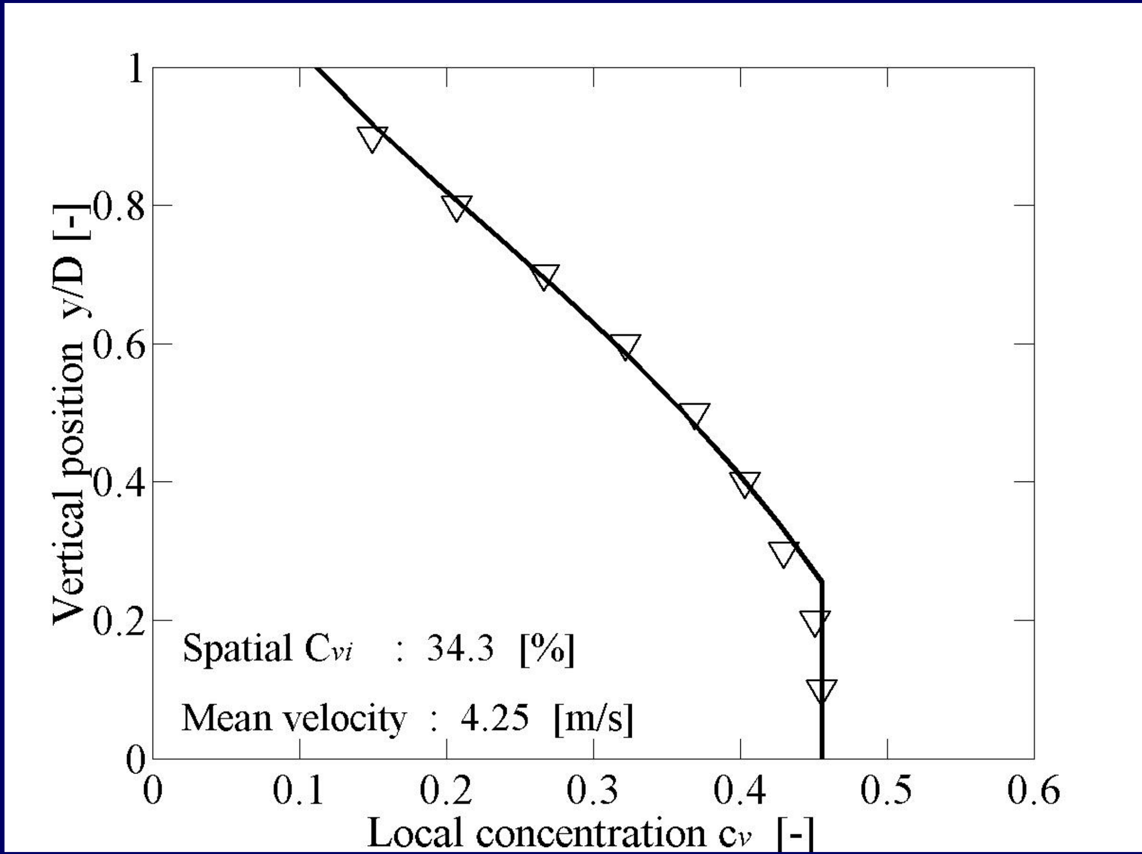

TU Delft

Particle-Liquid Interaction: Turb Dispersion

Turbulent diffusion model modified for hindered settling

The model is a balance of upwards and downwards solids fluxes composed of the volumetric settling rates and the diffusion fluxes:

The upwards flux per unit area = The downwards flux per unit area

gives

$$-\varepsilon_s \frac{dc_v}{dy} = v_{th}.c_v = v_t\left(1 - c_v\right)^m.c_v \quad \text{where} \quad \varepsilon_s = \frac{ML}{2}\tilde{v}'_y$$

and the integration must be carried out numerically (there is no analytical solution).

Example: Measured concentr'n profile

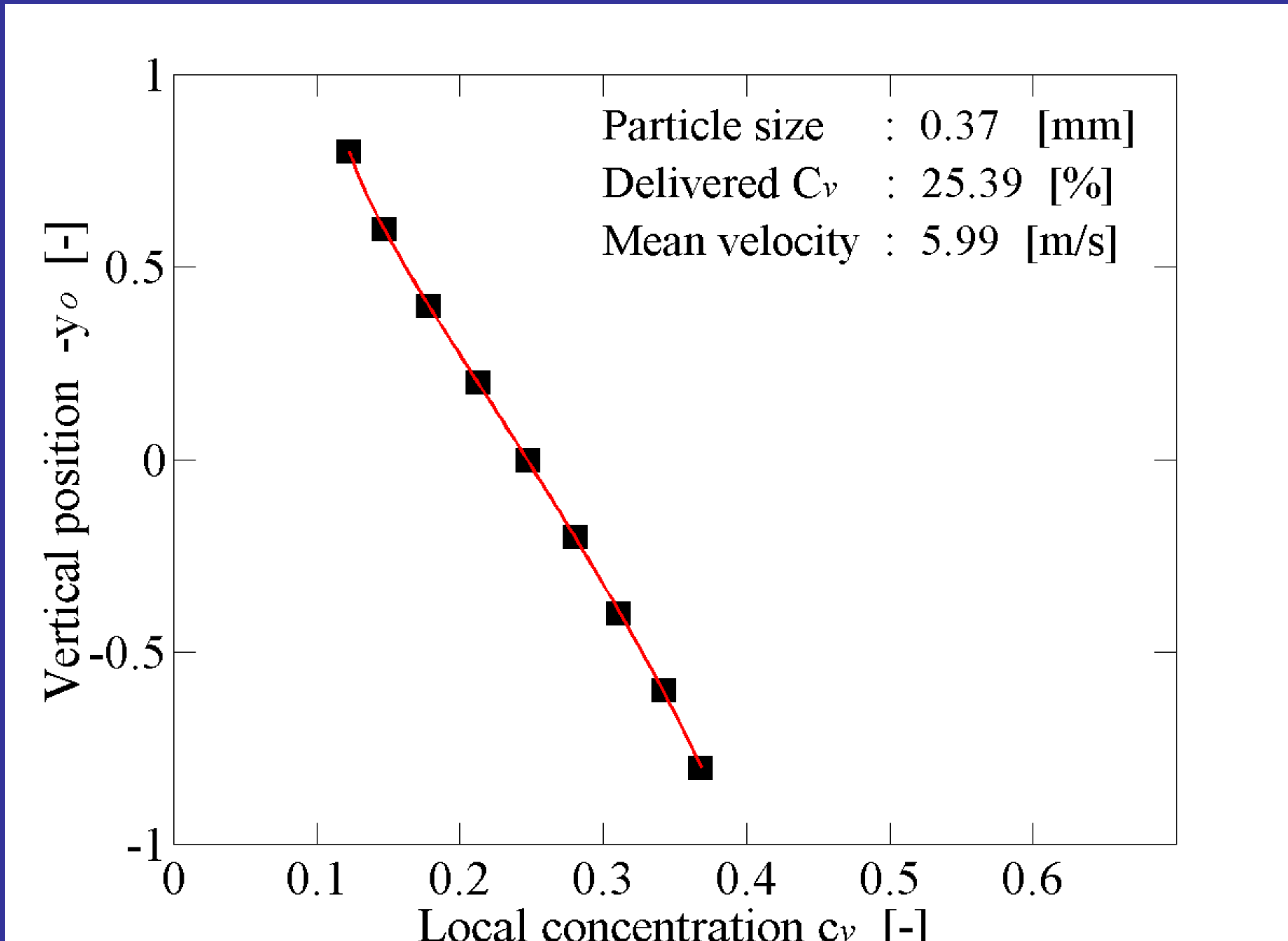

Example: Local solids dispersion coef.

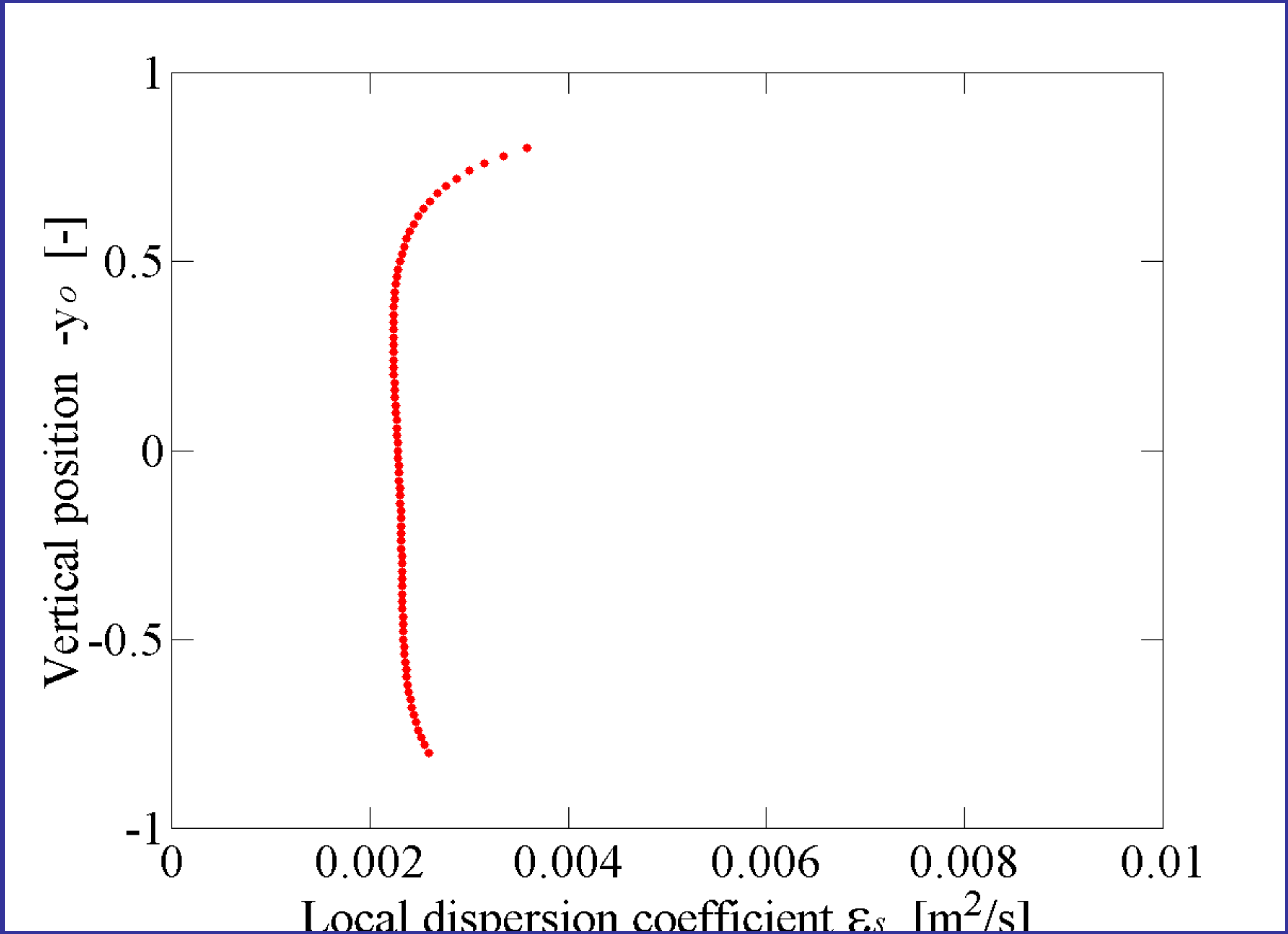

Example: Measured concentr'n profile

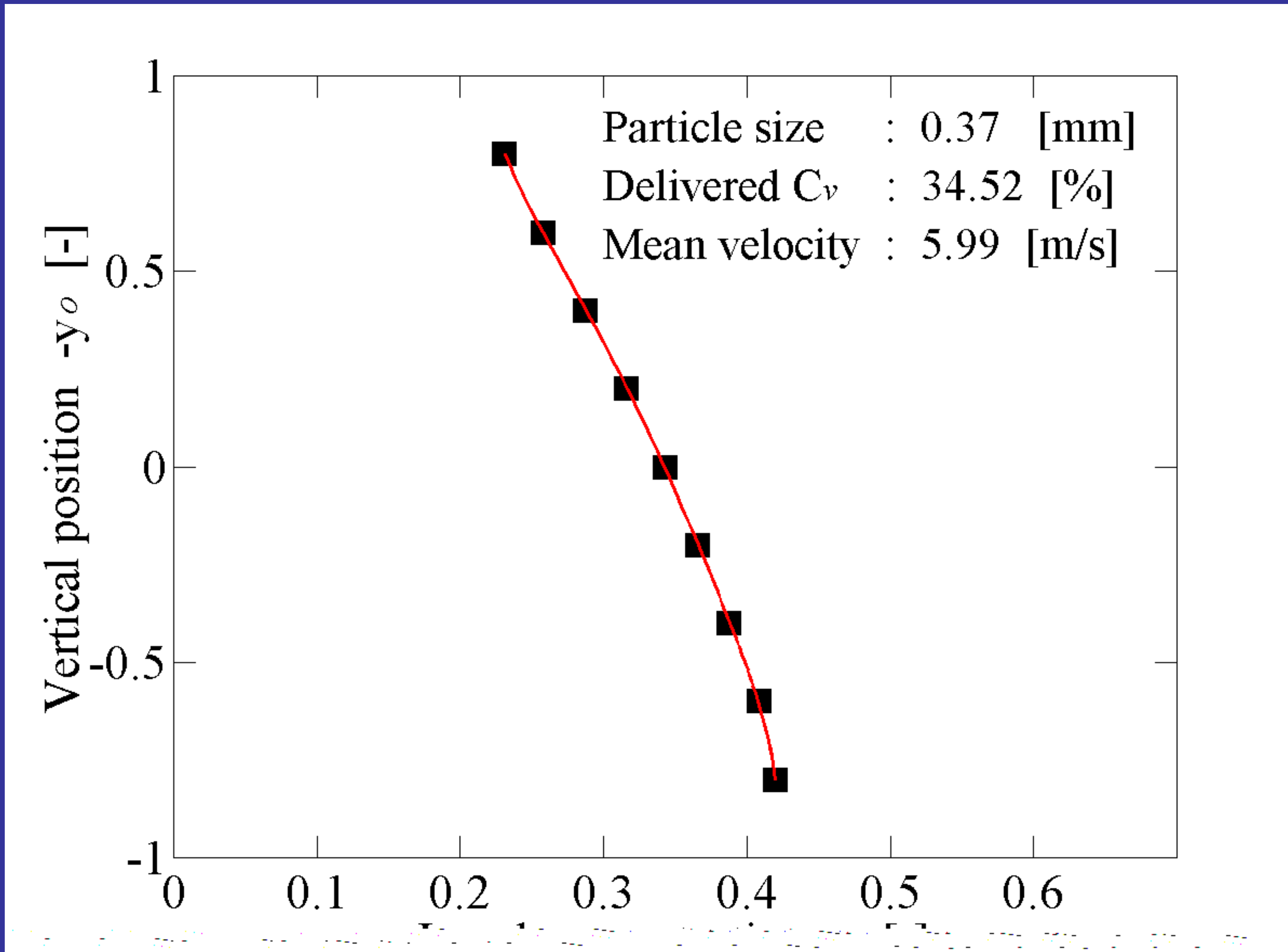

Example: Local solids dispersion coef.

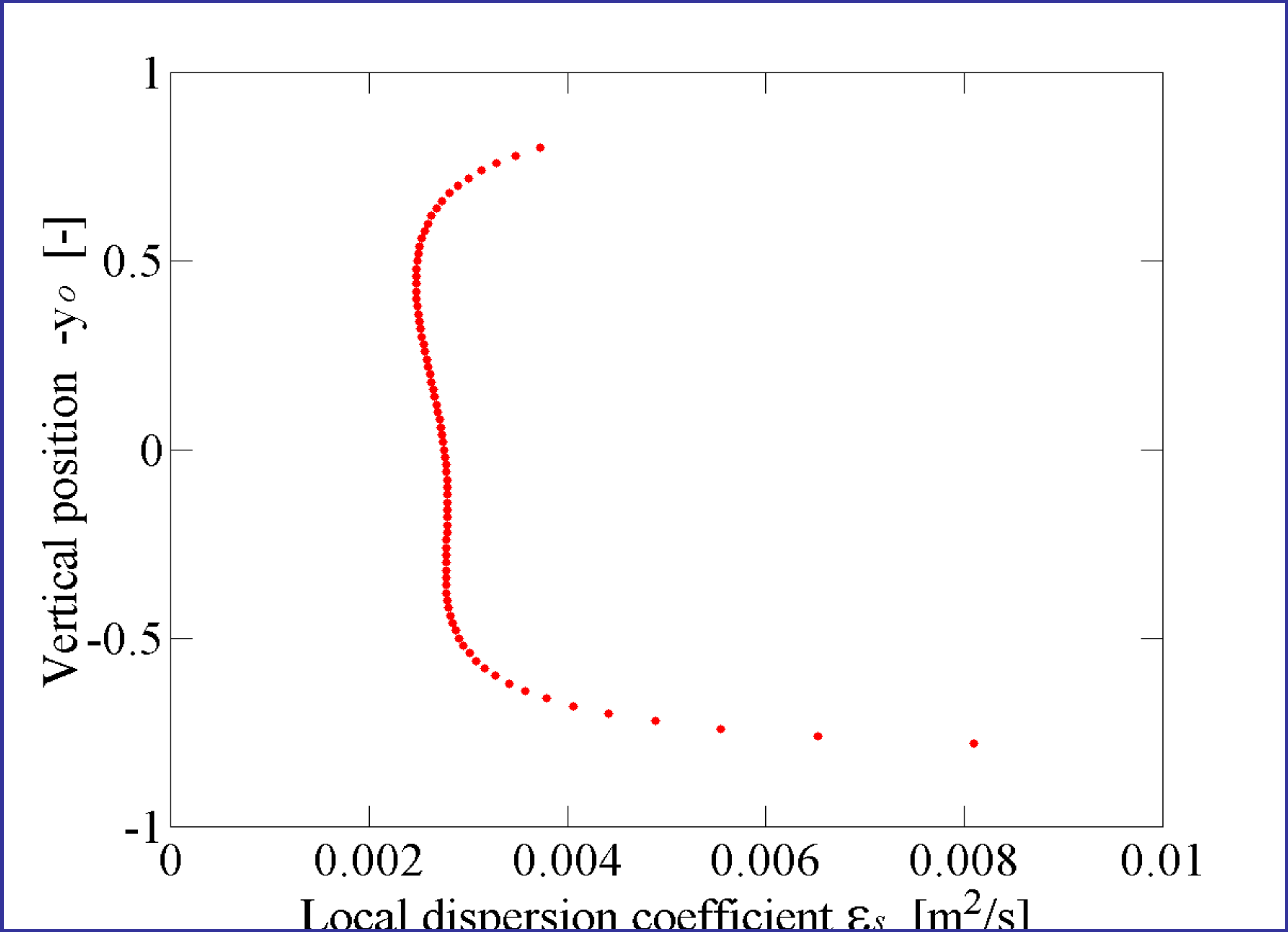

Example: Solids dispersion coefficient

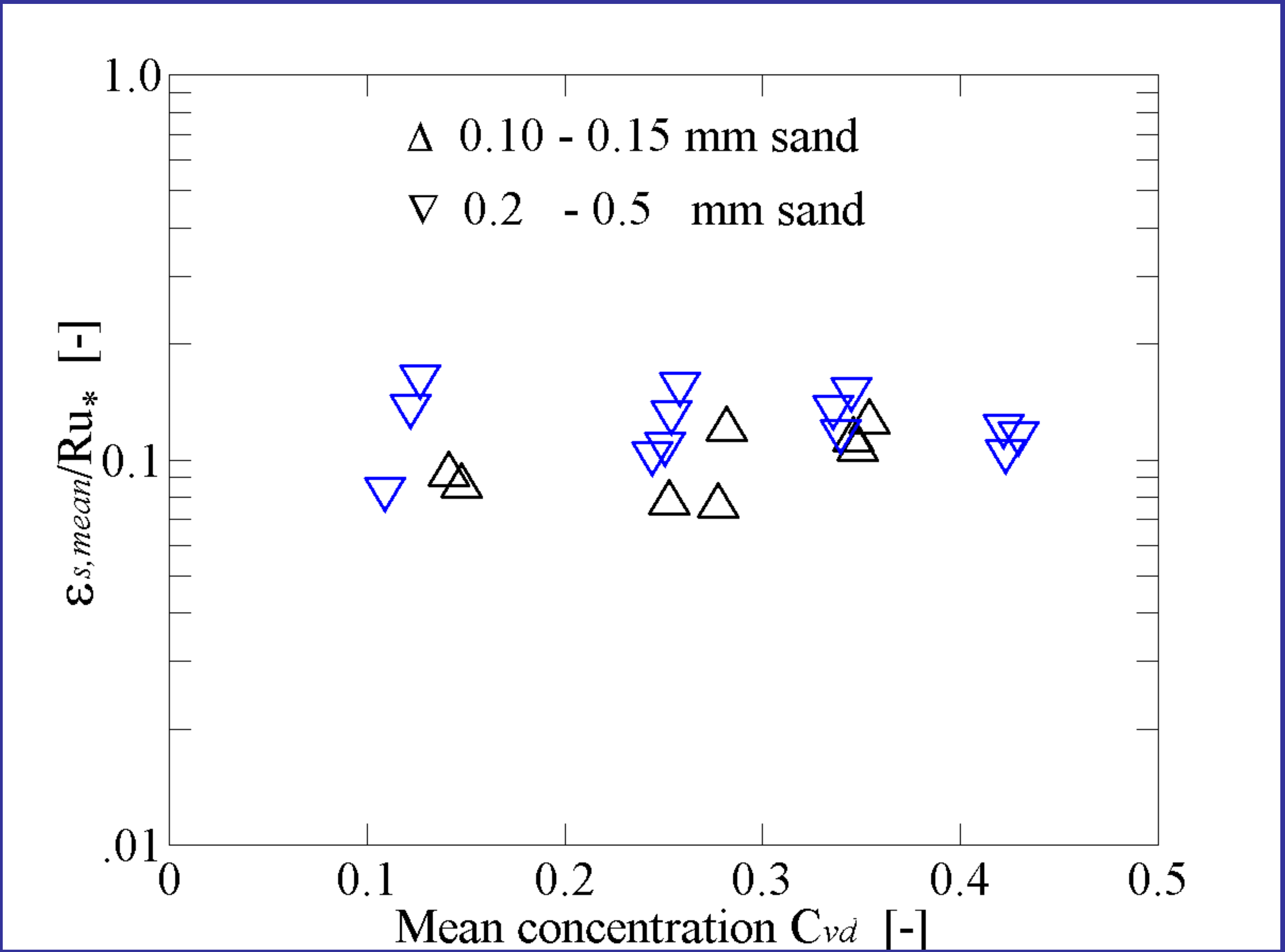

Particle-Particle Interaction: Contacts

Sand/gravel particles are transported in dredging pipelines often in a form of a *granular bed* sliding along a pipeline wall at the bottom of a pipeline. A mutual contact between particles within a bed gives arise to **intergranular forces** (i.e. stresses=force/area) transmitted throughout a bed and via a bed contact with a pipeline wall also to the wall.

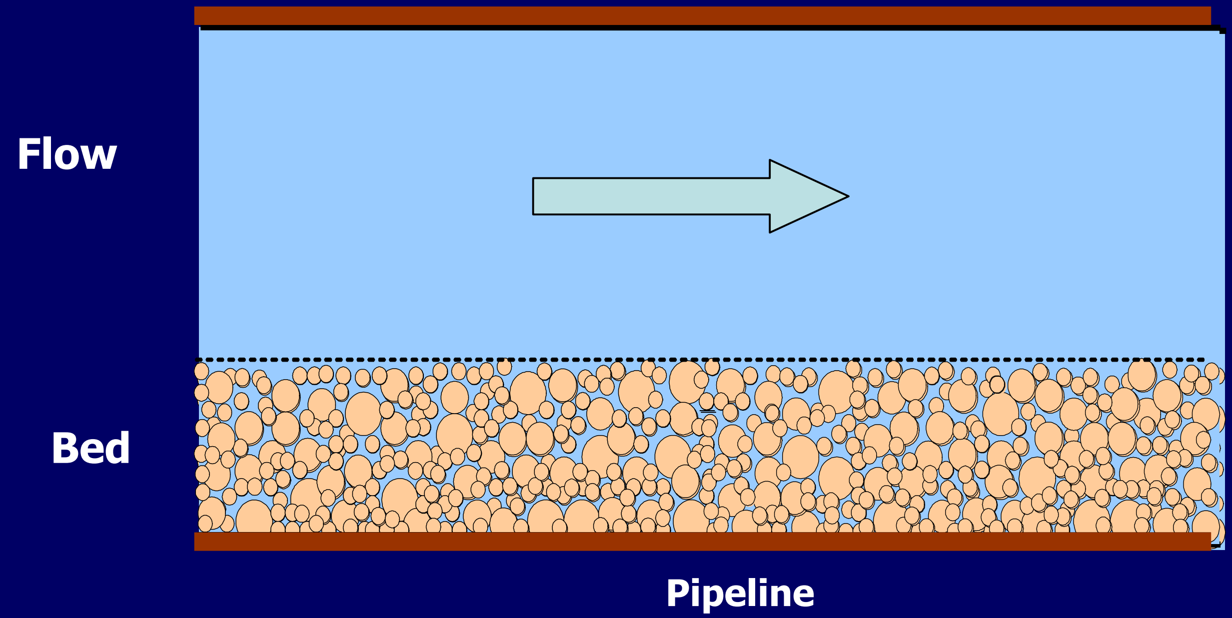

Particle-Particle Interaction: Contacts

DEM simulation of coarse slurry flow with particles in permanent contact, the granular bed slides *en bloc*.

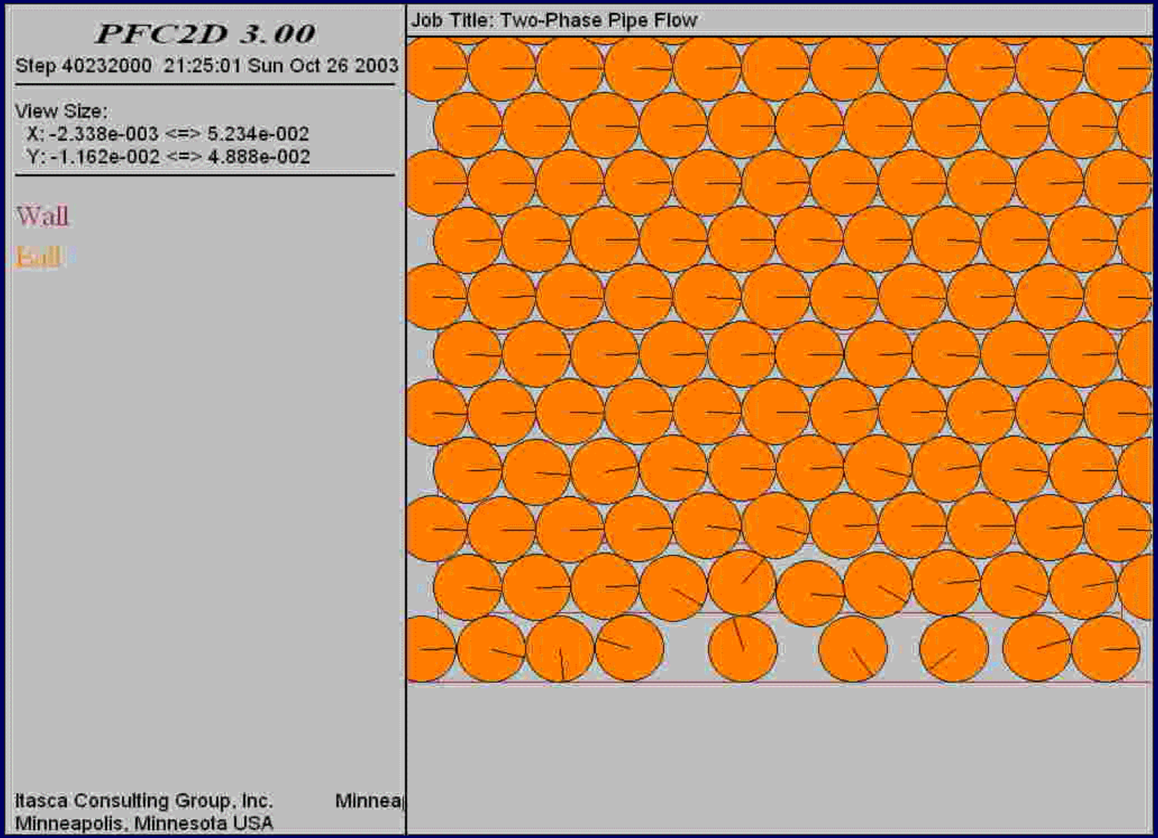

Particle-Particle Interaction: Contacts

The stress distribution in a granular body occupied by non-cohesive particles in continuous contact is a product of the weight of grains occupying the body. The intergranular stress has two components:

- an intergranular normal stress and
- an intergranular shear stress.

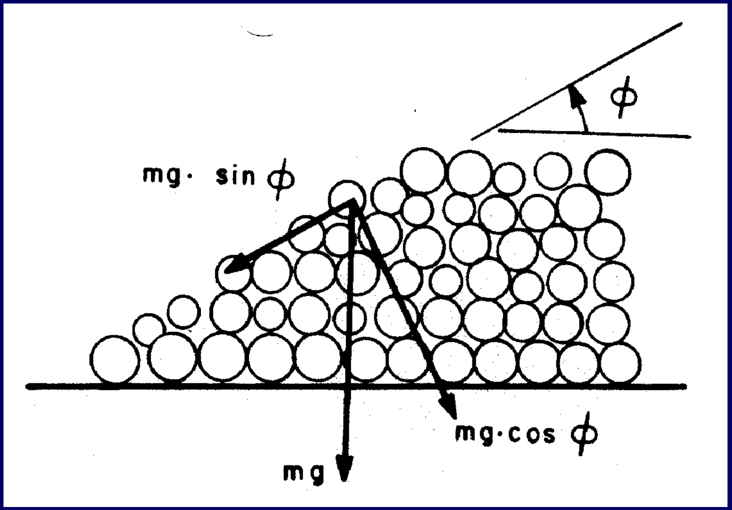

Particle-Particle Interaction: Contacts

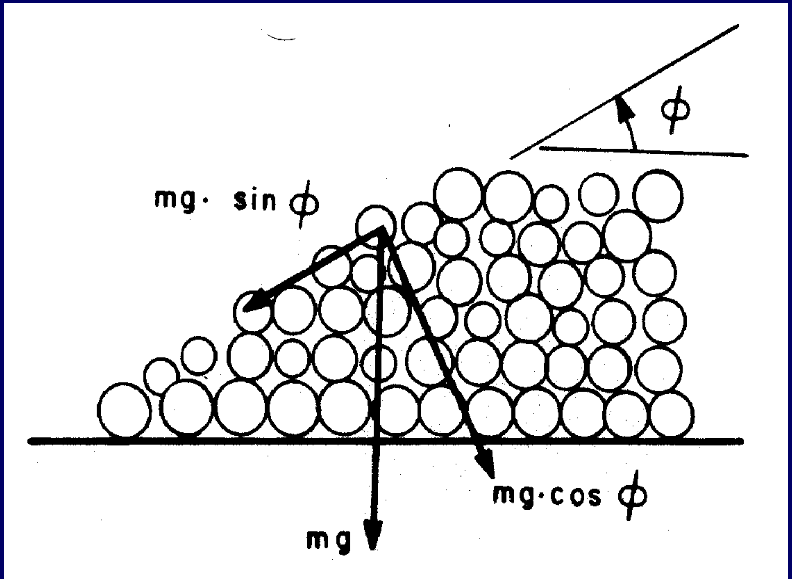

$$\tan\phi = \frac{\tau_s}{\sigma_s} = \frac{\tau_s}{\rho_f g (S_s - 1) C_{vb} H_s}$$

The intergranular stress has two components:

- intergranular normal stress and
- intergranular shear stress.

According to *Coulomb's law* these two stresses are related by the coefficient of friction. Du Boys (1879) applied Coulomb's law to sheared river beds. He related the normal stress and shear stress at the bottom of a flowing bed by the internal-friction coefficient (see eq.)

Particle-Particle Interaction: Collisions

Colliding particles in shear flow exercise also intergranular normal and shear stresses.

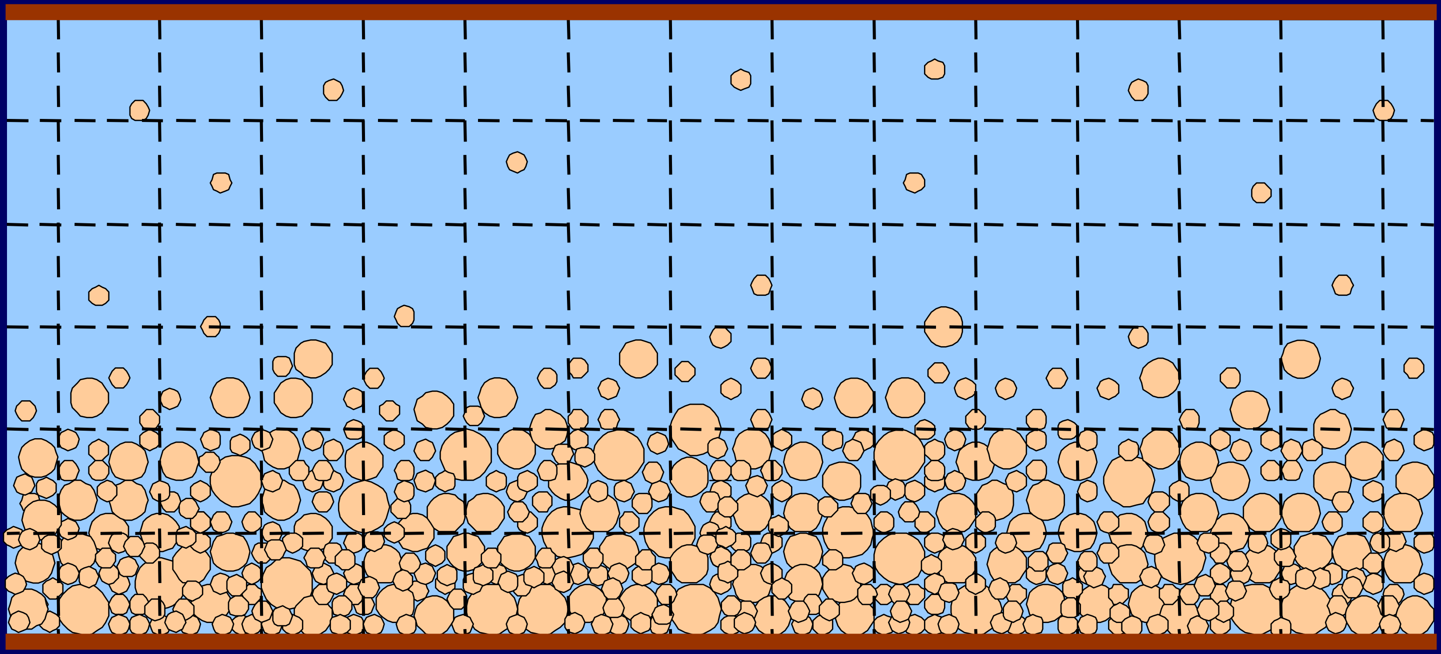

TU Delft

Particle-Particle Interaction: Collisions

DEM simulation of coarse slurry flow with colliding particles.

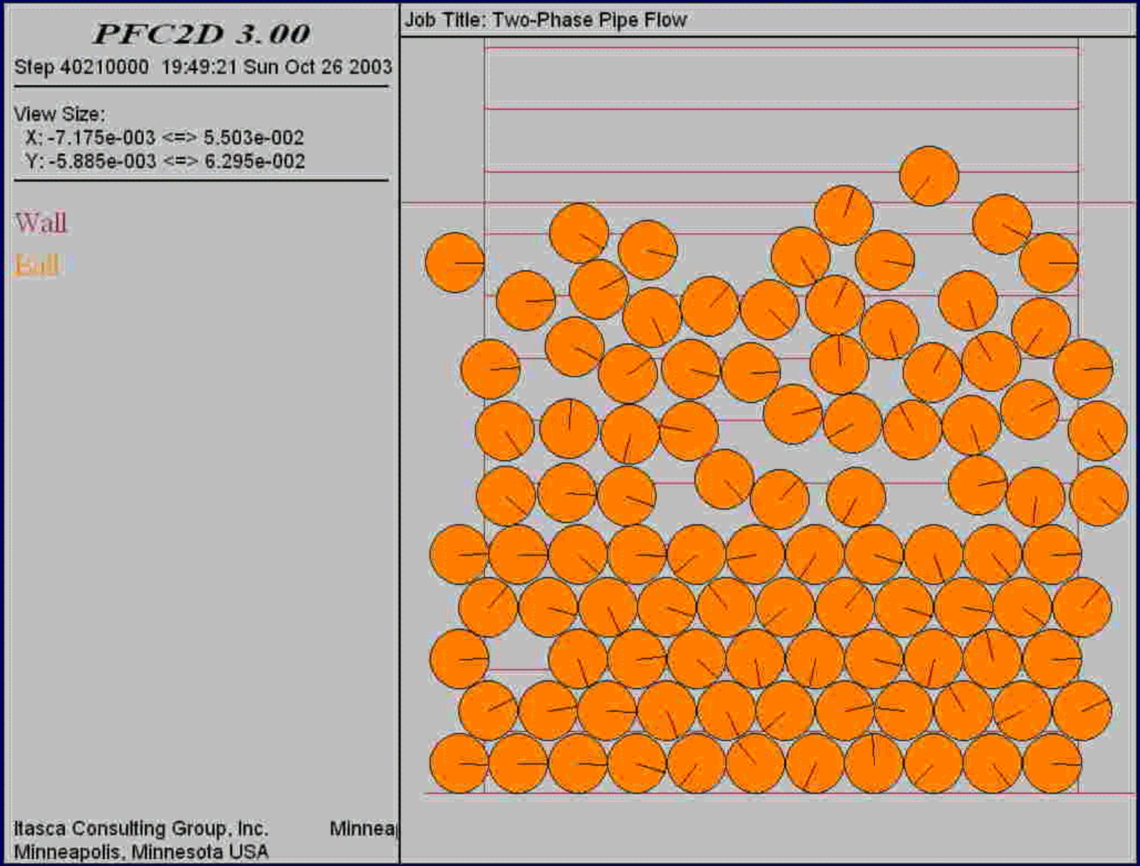

Particle-Particle Interaction: Collisions

$$\tan\phi' = \frac{\tau_{sb}}{\sigma_s}$$

The normal and shear stresses in a granular body experiencing the rapid shearing are related by using the coefficient of dynamic friction tanΦ' instead of its static equivalent tanΦ. Bagnold (1954,1956) measured and described the normal and tangential (shear) stresses in mixture flows at high shear rates (velocity gradients).

Bagnold's dispersive force is a product of intergranular collisions in a sheared layer rich in particles. The direction of the force is normal to the layer boundary on which it is acting.

Bagnold's experiment on collisional stress

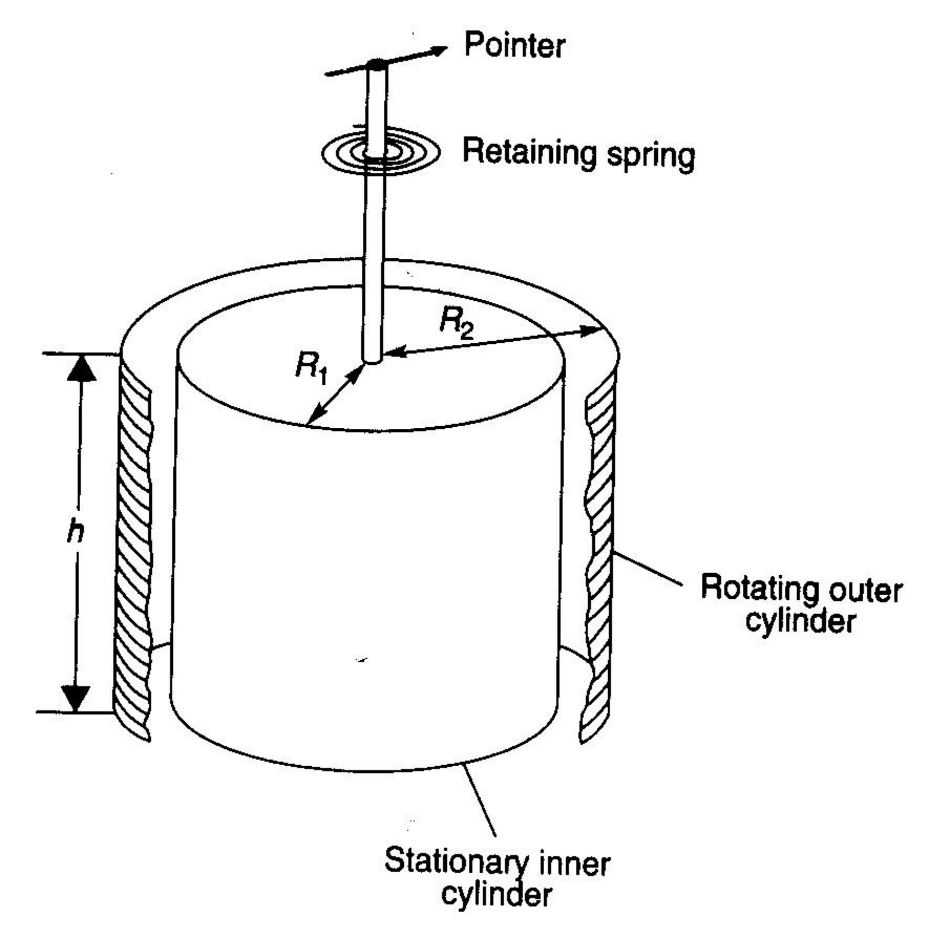

The classical rotational viscometer (see Fig.) was modified:

Rotating inner cylinder (RIC),

Stationary outer cylinder (SOC).

Measured:

- **Revolutions of RIC (Velocity gradient)**
- **Torque of RIC (Shear stress)**
- **Pressure at RIC wall (Normal stress)**